Stable seeder-injected Nd:YAG pulsed laser using a $RbTiOPO_4$ phase modulator

Junxuan Zhang (张俊旋)[1,2], Xiaolei Zhu (朱小磊)[1,*], Xiuhua Ma (马秀华)[1], Huaguo Zang (臧华国)[1], Shiguang Li (李世光)[1], Suyong Yin (殷苏勇)[1], and Weibiao Chen (陈卫标)[1]

[1]*Key Laboratory of Space Laser Communication and Detection Technology, Shanghai Institute of Optics and Fine Mechanics, Chinese Academy of Science, Shanghai 201800, China*

[2]*University of Chinese Academy of Sciences, Beijing 100049, China*

**Corresponding author: xlzhu@siom.ac.cn*

Received July 9, 2015; accepted September 10, 2015; posted online October 14, 2015

A stable, single-longitudinal-mode, nanosecond-pulsed Nd:YAG laser with a laser-diode dual-end pumping arrangement is constructed. Injection seeding is performed successfully by utilizing a $RbTiOPO_4$ crystal as the intracavity phase modulator to change the optical length of the slave cavity based on the delay-ramp-fire technique. The laser generates 9.9 mJ of pulse energy with a 16 ns pulse duration at a 400 Hz repetition rate. A near-diffraction-limit laser beam is achieved with a beam quality factor M^2 of approximately 1.2. The frequency jitter is 1.5 MHz over 2 min, and the fluctuation of the output pulse power is 0.3% over 23 min.

OCIS codes: 140.3570, 140.3580, 140.3540.

doi: 10.3788/COL201513.111404.

High peak power, nanosecond-pulsed Nd:YAG lasers operating in the single longitudinal mode (SLM) are of great utility in a variety of applications, such as laser spectroscopy, nonlinear optics, and differential absorption lidar (DIAL), and are useful as pumping sources for single-frequency optical parametric oscillators. For a single-frequency, nanosecond-pulsed laser, injection seeding is superior to traditional methods that use an interferometric longitudinal mode selector (e.g., inserting an etalon or grating), which usually results in significant power reduction or resonator alignment instability[1]. By injecting an external single-frequency seeder laser whose linewidth is much narrower than the axial mode separation of the high-gain oscillator cavity, the slave cavity can be prepopulated with photons from the seeder laser, and mode competition will lead to SLM operation within the slave cavity.

Successful seeder injection requires the slave cavity to be in resonance with the frequency of the seeder laser when the *Q*-switcher of the slave cavity is triggered. Until now, several methods have been designed to ensure the resonance condition, such as the build-up-minimizing technique[2], the ramp-and-fire technique[3], the ramp-hold-fire technique[4], and the delay-ramp-fire (DRF) technique[5]. In those techniques, the modulation of the optical path length of the slave cavity is usually carried out by two approaches: one uses a piezoelectric transducer to dither the rear mirror of cavity, and the other applies an intracavity electro-optic phase modulator. As we know, the latter offers several advantages, such as completely eliminating the mechanical moving of the rear mirror attached to the piezoceramic transducer (PZT), which solves the problem of the nonlinear moving of the electromechanical components, etc. The use of an intracavity electro-optic crystal phase modulator can achieve excellent frequency stability from a seeder-injected laser due to its precise feedback on the optical path length of the cavity.

In 2012, Moore *et al.* demonstrated SLM output from a Ti:sapphire ring laser using a KD_2PO_4 (KD*P) crystal to modify the optical phase of the seeder light propagating within the slave cavity[6]. In 2014, our group adopted an $LiNbO_3$ (LN) crystal as the intracavity phase modulator to realize the single-frequency-pulse laser output[7]. However, with a KD*P modulator, due to its lower electro-optic coefficients and refractive index, higher ramp voltage is needed to induce a sufficient phase change. What is more, the piezoelectric ringing effect of KD*P limits the maximum operating repetition rate of the SLM laser. With a LN phase modulator, its low damage threshold ($<250\ MW/cm^2$) limits the level of maximum output from the SLM laser. Compared with the KD*P and LN modulators, a $RbTiOPO_4$ (RTP) crystal has excellent optical properties: it is hydrolysis repellent, has high electro-optic coefficients, a high damage threshold ($>600\ MW/cm^2$), and lacks the piezoelectric ringing effect at an elevated repetition rate. It is believed that adopting a RTP phase modulator would be an effective method to obtain a higher pulse energy from a seeder-injected laser at an elevated repetition rate. In this Letter, we adopt a RTP crystal to modify the optical path length of the slave cavity based on the DRF technique. A stable nanosecond single-frequency pulse train with a high peak power, high power stability, high beam quality, and a high frequency stability was achieved at a 400 Hz repetition rate.

The schematic of the SLM laser setup is depicted in Fig. 1. It consists of three main parts: a continuous wave seeder laser, a *Q*-switched slave laser, and an electronic

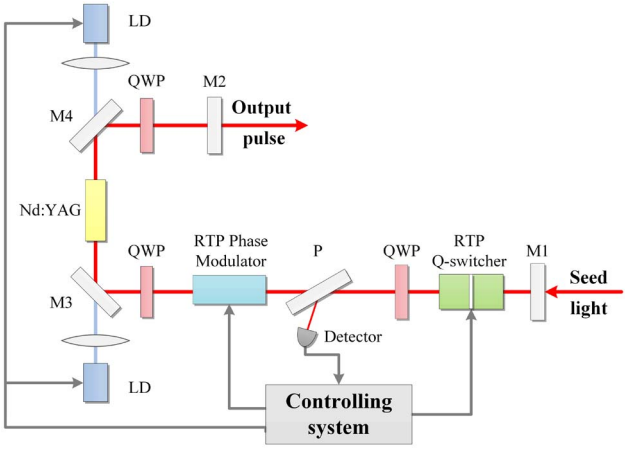

Fig. 1. Schematic diagram of single-frequency Nd:YAG laser.

control system. The seeder laser for injection seeding is a homemade non-planar ring oscillator Nd:YAG laser operating at 1064 nm with a maximum output of 350 mW[8].

The slave cavity is configured as a U-type arrangement allowing for p polarization oscillation[9]. The cavity length is approximately 450 mm, with an equivalent free spectral range (FSR) of 330 MHz. Two flat mirrors, M1 (rear mirror) and M2 (output coupler), each have a reflectivity of 95% and 40% at 1064 nm, respectively. M3 and M4 are two fixed dichroic mirrors, which have a high transmission coated at 808 nm and high reflection coated at 1064 nm. The gain rod is dual-end pumped by two laser diodes (LDs) with a maximum output peak power of 150 W for each. Two coupling lenses re-image the pump beam into a 1 mm-diameter spot inside the Nd:YAG crystal. The composite Nd:YAG crystal ($\Phi 4$ mm $\times$ 30 mm), which is designed to reduce the thermal lensing effect, includes a 20 mm 0.3% Nd^{3+}-doped YAG crystal sandwiched by two 5 mm undoped YAG crystals. In addition, a thermo-electric cooler is utilized to control the temperature of the composite Nd:YAG rod. Two cross-axis quarter-wave plates (QWPs) are inserted to create a "twisted mode" within the gain medium for spatial hole-burning elimination[10].

A total of three RTP crystals are utilized inside the slave cavity. A pair of RTP crystals (6 mm $\times$ 6 mm$\times$ 10 mm each), combined with a polarizer (P) and a QWP, act as an electro-optical Q-switcher[11]. This double-crystal structure [see Fig. 2(b)] is capable of compensating for the natural birefringence effect of the RTP crystal induced by the temperature variation. Another RTP is used to change the optical phase of the laser beam with no modification of the polarization, as illustrated in Fig. 2(a). Therefore, the polarization of the incident light must be parallel to the field-induced axis of the RTP. The effective change in the optical path length of the cavity, ΔL, as a function of the electric potential V, is given by

$$\Delta L = \Delta n_z L = n_z^3 \gamma_{33} V L / d / 2, \quad (1)$$

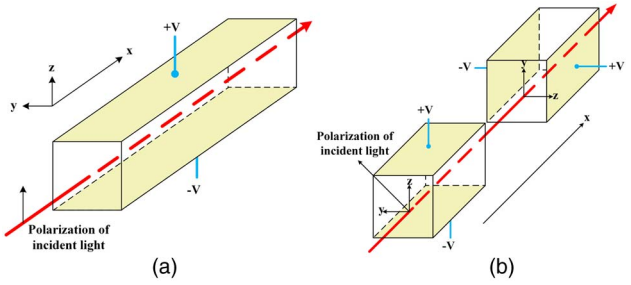

Fig. 2. RTP crystals used (a) as a phase modulator and (b) as a Q-switcher.

where n_z is the extraordinary refractive index of the RTP, γ_{33} is the electro-optic coefficient, L is the length of the RTP crystal, and d is the crystal's breadth. Specifically, an RTP crystal with a size of $L = 35$ mm and $d = 4$ mm is used in our experiments. In order to ensure the precise detection of the resonance peaks, approximately 1500 V of electric potential is used to generate 2.6 times the FSR of the cavity. For the same-size KD*P modulator, more than 3530 V of voltage should be applied to generate the same change in the optical length. Such a high voltage leads to more difficulty in constructing the circuit.

In this experiment, the DRF technique is selected for seeder injection. The electronic units for feedback control are designed to match one longitudinal mode of the slave cavity to the frequency of the seeder. The DRF process was started by triggering the LDs' drivers, which generated a pump pulse. A voltage ramp was then amplified and applied to the RTP crystal based on the suitable time delay of the Q-switcher. The interference pattern, detected by a photodiode, was produced by the seeder light reflecting off the polarizer. Once the resonance peak was detected, a transistor-transistor logic (TTL) trigger was then generated and sent to the driver of the Q-switcher to fire the pulsed laser. This finally resulted in single frequency emission. Figure 3 shows the DRF event timing signals. Here, we added an extra feedback system by adjusting the beginning time of the ramp voltage to maintain a constant delay between the pump pulse and the Q-switcher trigger signal, which favors a good immunity of the output energy fluctuation.

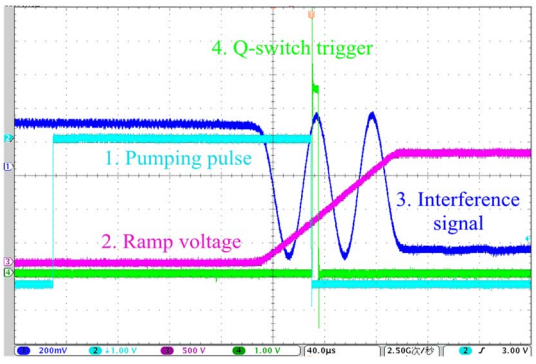

Fig. 3. Timing diagram of signals in DRF event.

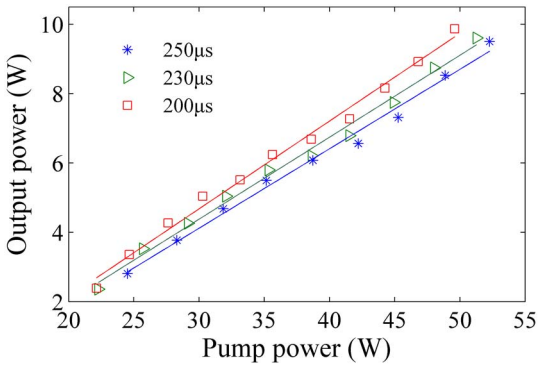

Fig. 4. Laser output energy verse pump-pulse energy with different pump-pulse durations.

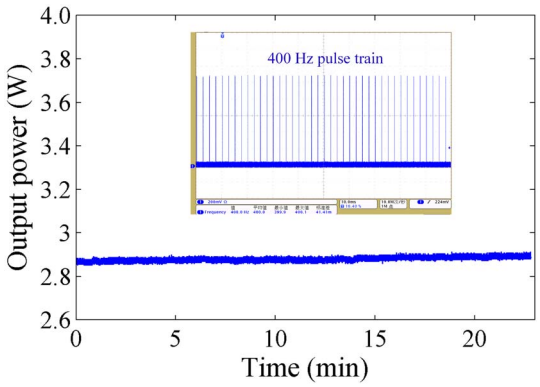

Fig. 6. Laser pulse power stability over 23 min.

Figure 4 illustrates the experimental results of the output power variation with different pump pulse widths at the repetition rate of 400 Hz. It reveals that a pump pulse with a narrower duration is helpful to increase the optical–optical conversion efficiency. At a certain repetition rate, a narrower pump pulse width decreases the duty ratio of the pump input, so the extra loss induced by the thermal effect will decrease, and higher optical–optical conversion efficiency can be achieved. Hence, all the following experiments were carried out with a 200 μs pump-pulse duration at a repetition rate of 400 Hz.

The output pulse energy and the pulse width of the seeder-injected laser as a function of the pump-pulse energy are shown in Fig. 5. The laser pulse width decreases as the pump-pulse energy increases. The laser pulse width is relative to the cavity length, the round-trip loss, and the gain in the cavity. A higher gain would lead to a narrower pulse width. At last, up to 9.9 mJ of pulse energy output was obtained when the pump pulse was increased to 49.6 mJ, corresponding to an optical–optical conversion efficiency of 20% and a slope efficiency of 25%. The maximum pulse energy was increased to more than two times as large as that obtained from a SLM laser using the LN crystal as the phase modulator. Since the pulse width is approximately 16 ns, a maximum output peak power of 619 kW was achieved. In order to avoid optical damage in a routine operation, an output pulse energy of 7.2 mJ was chosen to measure the following parameters.

The power variation of this seeder-injected laser was recorded by a power meter and is displayed in Fig. 6. In an interval of 23 min with a 16.8 W pump incidence, the mean value of laser output power was 2.88 W. A standard deviation of 9 mW was derived, and 0.3% of output power fluctuation was achieved. The inset of Fig. 6 shows the pulse train recorded by an oscilloscope.

The measured laser beam quality of M^2 is shown in Fig. 7. Beam quality factors M^2 of 1.18 in the horizontal direction and 1.21 in the vertical direction were obtained. The inset in Fig. 7 presents the near-field intensity distribution of the laser beam spot, which illustrates a near-diffraction-limited beam with good Gaussian distribution.

The effect of successful injection seeding is readily observable in the temporal pulse shape, which was detected by a 500 MHz bandwidth photodiode and recorded by a Tektronix DPO 4104B oscilloscope with a bandwidth of 1 GHz. With successful injection seeding, the pulses show a smooth trace, as is expected for a single-mode operation [see Fig. 8(a)], otherwise, serious modulation is exhibited in the pulse temporal profile because of the

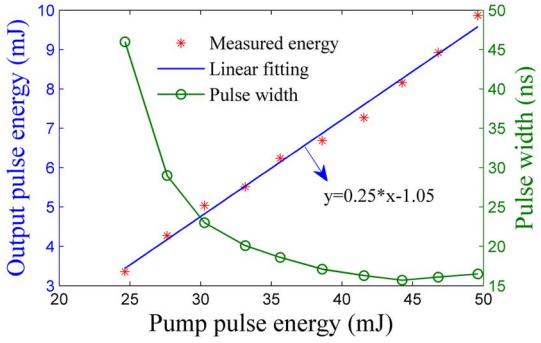

Fig. 5. Laser output energy and pulse duration as a function of the pump-pulse energy.

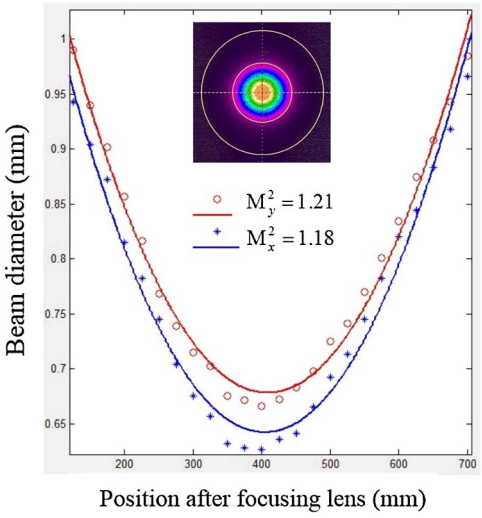

Fig. 7. Measurement of beam quality factor M^2.

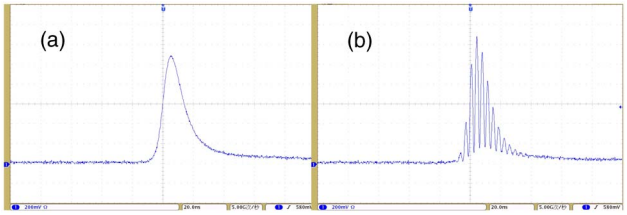

Fig. 8. Temporal trace of laser pulse (a) with and (b) without seeder injection.

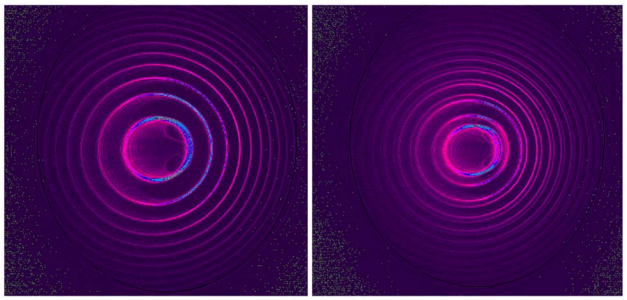

Fig. 9. Spectrum interference pattern (a) with and (b) without seeder injection.

multi-mode beating [see Fig. 8(b)]. The spectral characteristics of the laser pulse were also analyzed by a Fabry–Perot interferometer with a gap of 120 mm, and exhibited a reflectivity of 95% at 1064 nm. The recorded interference patterns are shown in Fig. 9. When a single-mode emission was realized, only one set of interference patterns was detected, as shown in Fig. 9(a). But once the seeder injection failed, multiple sets of interference patterns would occur, as shown in Fig. 9(b)[12]. Furthermore, the optical heterodyne technique was adopted to measure the spectral linewidth of the single-mode operation; a linewidth of 43 MHz was achieved. The longitudinal mode separation of the cavity was 330 MHz. It is clear that single-longitudinal-mode output was obtained.

A High Finesse WS/7 IR Wavelength Meter with a spectral linewidth resolution limit of 120 MHz at 1064 nm was used to measure the frequency stability of this seeder-injected laser. The spectral frequency stability over 37 min is illustrated in Fig. 10. A standard deviation of 5.7 MHz could be derived. As a comparison, the frequency stability of 1.5 MHz over 2 min is also shown in the inset of Fig. 10. In our previous work using the same slave cavity arrangement, 1.7 MHz (rms) of frequency stability was achieved by using a LN crystal as an intracavity phase modulator[7], but only 3.5 MHz (rms) of frequency stability was realized by using a PZT to feedback the cavity length over 2 min[13]. The experimental results demonstrated that better spectrum performance could be achieved from an injection-seeded laser by adopting an intracavity optical phase modulator consisting of an RTP crystal.

As a comparison, the laser performance was also studied when 900 V of voltage was applied to the RTP crystal.

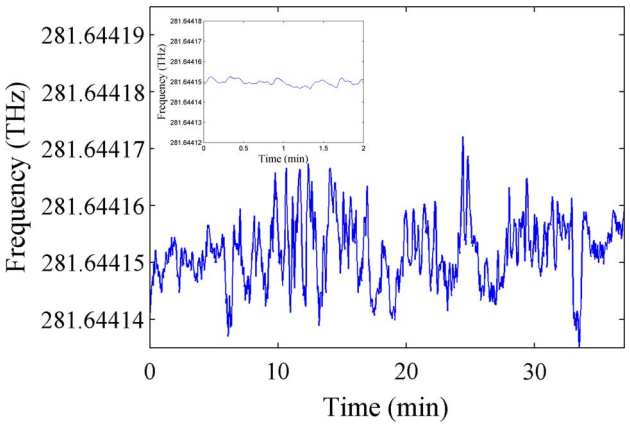

Fig. 10. Frequency stability over 37 min with 1500 V of ramp voltage.

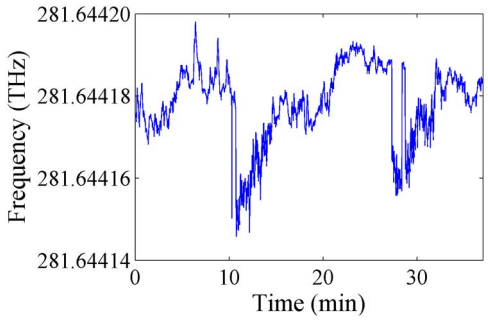

Fig. 11. Frequency stability over 37 min with 900 V of ramp voltage.

The measured laser parameters were almost the same as the above results except for the long-term frequency stability, which decreased to 9.3 MHz over 37 min (shown in Fig. 11). As we know, when the ramp voltage applied to the RTP was decreased to 900 V, only 1.5 times the FSR was generated for detecting the resonance peaks. The reason for the larger fluctuation of the output frequency was that the extract of the Q-switch trigger was not always at the peak of the interference signal, namely the best cavity length, which was resonant with the seed laser. A good way to improve the extraction accuracy of the circuit is to increase the number of the FSR to decrease the difficulty of controlling the circuit. Hence, increasing the length of the electro-optical phase modulator and increasing the voltage applied to the crystal are two effective methods to improve the long-term frequency stability.

In conclusion, an seeder-injected, single-frequency, nanosecond-pulsed Nd:YAG laser with a RTP electro-optic crystal intracavity phase modulator is developed, and a stable SLM operation is successfully demonstrated. Combined with a double-crystal RTP Q-switcher, a laser output pulse energy up to 9.9 mJ is obtained at a repetition rate of 400 Hz. In this experimental arrangement, a stable SLM operation with a maximum output power of 6.75 W is also achieved when the repetition rate is

increased to 900 Hz. This seeder-injected laser is capable of generating a stable SLM laser output with high power stability, high beam quality, and high frequency stability. It is believed to be a good candidate for laser spectroscopy and DIAL applications.

This work was partly supported by the Natural Science Foundation of Shanghai under Grant No. 12ZR1435100.

References

1. Y. K. Park, G. Giuliani, and R. L. Byer, IEEE J. Quantum Electron. **20**, 117 (1984).
2. L. A. Rahn, Appl. Opt. **24**, 940 (1985).
3. S. W. Henderson, E. H. Yuen, and E. S. Fry, Opt. Lett. **11**, 715 (1986).
4. T. Walther, M. P. Larsen, and E. S. Fry, Appl. Opt. **40**, 3046 (2001).
5. Z. Jun, Z. Huaguo, Y. Ting, L. Jiqiao, and C. Weibiao, Proc. SPIE **6681**, 66810R (2007).
6. T. Z. Moore and F. S. Anderson, Proc. SPIE **8235**, 82351M (2012).
7. J. Zhang, X. Zhu, H. Zang, X. Ma, S. Ying, S. Li, and W. Chen, Appl. Opt. **53**, 7241 (2014).
8. R. Zhu, J. Zhou, J. Liu, D. Chen, Y. Yang, and W. Chen, Chin. J. Lasers **38**, 1102011 (2011).
9. Q. Yang, X. Zhu, J. Ma, T. Lu, X. Ma, and W. Chen, Chin. Opt. Lett. **13**, 021402 (2015).
10. V. Evtuhov and A. E. Siegman, Appl. Opt. **4**, 142 (1965).
11. J. Huang, X. Hu, and W. Chen, Chin. Opt. Lett. **13**, 061401 (2015).
12. M. Gao, F. Yue, T. Feng, J. Li, and C. Gao, Chin. Opt. Lett. **12**, 021404 (2014).
13. J. Wang, R. Zhu, J. Zhou, H. Zang, X. Zhu, and W. Chen, Chin. Opt. Lett. **9**, 081405 (2011).